Efficient Room-Temperature Operation of a Quantum Dot Spin-Polarized Light-Emitting Diode under High-Bias Conditions

Kohei Etou, Satoshi Hiura,* Soyoung Park, Junichi Takayama, Agus Subagyo, Kazuhisa Sueoka, and Akihiro Murayama

Faculty of Information Science and Technology, Hokkaido University, Sapporo 060-0814, Japan

(Received 20 June 2022; revised 12 September 2022; accepted 20 January 2023; published 21 February 2023)

Spin-polarized light-emitting diodes (spin LEDs) are essential for the optical transfer of carrier-spin information in spin-based electronic circuits. Efficient operation under high-bias conditions is required for high-speed transfer of spin information and strong light emission. However, achieving high-electroluminescence (EL) circular polarization is hampered by electric-field-induced spin relaxation during drift transport in undoped GaAs barriers. Herein, we demonstrate the efficient room-temperature operation of a spin LED using (In,Ga)As quantum dots (QDs) tunnel coupled with a 5-nm-thick Ga(N,As) quantum well (QW). A high-EL circular polarization of approximately 7% is achieved, even under high-bias conditions, in comparison with the lower value of approximately 3% for the conventional QD spin LED without Ga(N,As). This is realized by an increase of spin polarization after injection into the QDs by utilizing remote spin filtering of QD electrons via an adjacent tunnel-coupled Ga(N,As) QW. These results demonstrate that the tunnel-coupled structure of (In,Ga)As QDs and Ga(N,As) QW is a promising active layer of spin LEDs for achieving both strong EL emission and high-EL circular polarization at room temperature.

DOI: 10.1103/PhysRevApplied.19.024055

I. INTRODUCTION

To support an advanced information society, the electric power consumption required for enormous information processing must be reduced. However, reducing the number of information carriers has the fundamental problem of reducing the signal-to-noise ratio of signals. Therefore, there has been increasing interest in developing an alternative paradigm for future information technologies [1]. The quantum states of photons and electrons can be used to provide information to a very small number of photons and electrons. These quantum states are the circular polarization properties of light and the spin of electrons. The photoelectric conversion of semiconductors can be directly achieved according to the angular momentum conservation law [2].

Spin-polarized light-emitting diodes (spin LEDs) based on III-V semiconductors are known as spin-photon conversion devices. Significant advances have been made over the past two decades in understanding spin injection [3–12], spin relaxation [13–15], and spin transport [16,17] in spin LEDs. III-V semiconductor quantum dots (QDs) are the most promising candidates for optically active layers because of their suppressed carrier-spin relaxation [18–20], in addition to the high efficiency of optical transitions [21,22]. Recently, a high degree of electroluminescence (EL) circular polarization of approximately 8% was achieved at room temperature using (In,Ga)As QDs capped with a *p*-doped GaAs barrier [17], which can suppress the D'yakonov-Perel' (DP) spin relaxation that is dominant at high temperatures [23]. However, the EL circular polarization significantly decreases to less than 3% under high-bias conditions, owing to the enhancement of electric-field-induced DP spin relaxation in the undoped GaAs barriers [17]. To achieve both high-speed transfer of electron-spin information and efficient spin-photon conversion, a higher EL circular polarization under high-bias conditions is desirable.

Here, we briefly introduce the basic principle of the defect-engineered spin-filtering effect in dilute nitride, Ga(N,As), which is the key function in this study. Under electrical spin injection or circularly polarized optical excitation, even a slight spin polarization of conduction-band electrons can result in a dynamic spin polarization of the electrons localized at the spin-filtering defects via a spin-dependent recombination (SDR) process [24]. The SDR process drives both conduction-band electrons and defect electrons towards the majority-spin orientation. The resulting spin-polarized defects in Ga(N,As) can selectively capture conduction-band electrons with opposite spin directions (minority spins), owing to Pauli blocking, thereby enhancing the spin polarization of conduction-band electrons. Recently, a tunnel-coupled structure of QDs and

*hiura@ist.hokudai.ac.jp

Ga(N,As) demonstrated an extremely high electron-spin polarization of 90% at room temperature [25]. This achievement is accomplished by the combination of the preferential injection of majority spins from Ga(N,As) to QDs, and the back transfer of minority spins from QDs to Ga(N,As). The higher quasi-Fermi level for majority spins in Ga(N,As) drives this characteristic spin filtering [25]. In this study, we fabricate spin LEDs using (In,Ga)As QDs tunnel coupled with a Ga(N,As) quantum well (QW). The bias dependence of EL circular polarization is primarily studied at room temperature. A high-EL circular polarization of approximately 7% is achieved over a wide bias range, including high-bias conditions, in comparison with the lower value of approximately 3% for the QD spin LED without Ga(N,As). We find that the spin polarization of QD electrons, despite decreasing during their transit across an undoped GaAs barrier, can be recovered after injection into QDs via the spin-filtering effect of Ga(N,As).

II. EXPERIMENTAL DETAILS

Figure 1(a) shows a schematic of a QD spin LED. The semiconductor part is grown by molecular beam epitaxy, whereas the MgO tunneling barrier and ferromagnetic Fe electrode are grown by electron-beam deposition. The semiconductor structure consists of p-GaAs:Zn (100) substrate ($p = 1 \times 10^{19}$ cm^{-3})/300-nm p-GaAs:Be ($p = 1 \times 10^{18}$ cm^{-3})/100-nm p-$Al_{0.3}Ga_{0.7}As$:Be ($p = 1 \times 10^{18}$ cm^{-3})/active layer/50-nm undoped GaAs/50-nm n-$Al_{0.3}Ga_{0.7}As$:Si ($n = 2 \times 10^{17}$ cm^{-3})/5-nm n-GaAs:Si ($n = 5 \times 10^{18}$ cm^{-3}). The active layer is composed of three layers of (In,Ga)As QDs tunnel coupled with a 5-nm-thick Ga(N,As) QW. The Ga(N,As) QW is grown on a 30-nm-thick GaAs layer at 400 °C using a radio-frequency (rf) plasma source for nitrogen. Subsequently, 3.8-monolayer- (ML) thick (In,Ga)As QDs are grown at 480 °C after the growth of a 3-nm-thick GaAs tunneling barrier and capped with 10-nm-thick undoped GaAs. The nitrogen content of the Ga(N,As) QW is set to 0.9% by adjusting the growth conditions of the rf power and N_2 flow rate, leading to a resonant energy alignment between the ground state (GS) of the (In,Ga)As QD and Ga(N,As) QW [see Fig. 1(b)]. The nitrogen content is roughly determined by secondary-ion mass spectrometry from three layers of 20-nm-thick Ga(N,As) grown under the same conditions (Fig. S1 within the Supplemental Material [26]). An areal QD density of 3.2×10^{10} cm^{-2}, an average QD diameter of 22 nm, and a QD height of 4 nm are estimated by atomic force microscopy and transmission electron microscopy of reference QDs (Figs. S2 and S3 within the Supplemental Material [26]). The growth of the Fe/MgO spin injector was described previously [17]. The LED device is fabricated using standard photolithography and etching techniques, and no noticeable leakage current is detected. The contact area on the device is 0.35×0.35 mm^2.

Circularly polarized EL spectra are obtained by mounting the spin LED device in a superconducting-magnet cryostat with magnetic fields up to 5 T perpendicular to the sample plane. The injection current is varied from 30 to 100 mA, which corresponds to an applied bias voltage of 2.3–3.1 V. The EL signals are detected using a cooled (In,Ga)As detector with Faraday geometry. The circular polarization degree (CPD) of EL tracks the simplified hard-axis magnetization curve of Fe (not experimental data) with a saturation field of 2.2 T [5], as shown in Fig. 1(c). The magnetic-field-induced linear background is subtracted from the measured CPD values, according to a previous study [17]. Furthermore, circularly polarized photoluminescence (PL) measurements with bias voltage are performed under pulsed σ^+-polarized excitation. A wavelength-tunable pulsed laser with a repetition rate of 80 MHz and pulse width of less than 120 fs is used as the excitation source. The excitation power is varied from 1 to 20 mW. The excitation energy is tuned to 1.46 eV for optically generating electron-spin polarization in undoped GaAs barriers, where the spin-polarization degree is expected to be 50%, according to the optical-transition selection rule [2]. The CPD of EL and PL are analyzed through a combination of a quarter-wave plate and linear polarizer. CPD is defined as $(I_{\sigma+} - I_{\sigma-})/(I_{\sigma+} + I_{\sigma-})$, where $I_{\sigma\pm}$ denotes the $\sigma^{\pm}$-polarized emission intensity. The CPD measured in QDs reflects the electron-spin polarization in the QD emissive states [17,25]. All the experiments are performed at 295 K.

III. RESULTS AND DISCUSSION

Figure 1(b) shows a three-dimensional calculation of the band profiles for the tunnel-coupled structure of the (In,Ga)As QD and 5-nm-thick Ga(N,As) QW with no electric field. All calculations are performed using the simulator nextnano [27]. The In composition of the QD is set to 0.62 to match the EL emission energy of approximately 1.06 eV, as described in Figs. 3(a) and 3(b). The nitrogen content of the Ga(N,As) QW is set at 0.9%. The calculation model assumes a 1-nm-thick wetting layer and one truncated pyramidal QD with a base length of 22 nm and height of 4 nm, considering the uniform In composition inside the QD and the influence of strain on the local band structure. The electron GS of the Ga(N,As) QW is well aligned with that of the (In,Ga)As QD, which leads to a coupled wave function between the QD and Ga(N,As). In this situation, electrons can transfer between the QD and Ga(N,As) via spin-conserving tunneling. This nanosystem enables the amplification of electron-spin polarization in QDs via the selective removal of minority spins from the QDs to a Ga(N,As) spin filter [25], which is the key function in this study.

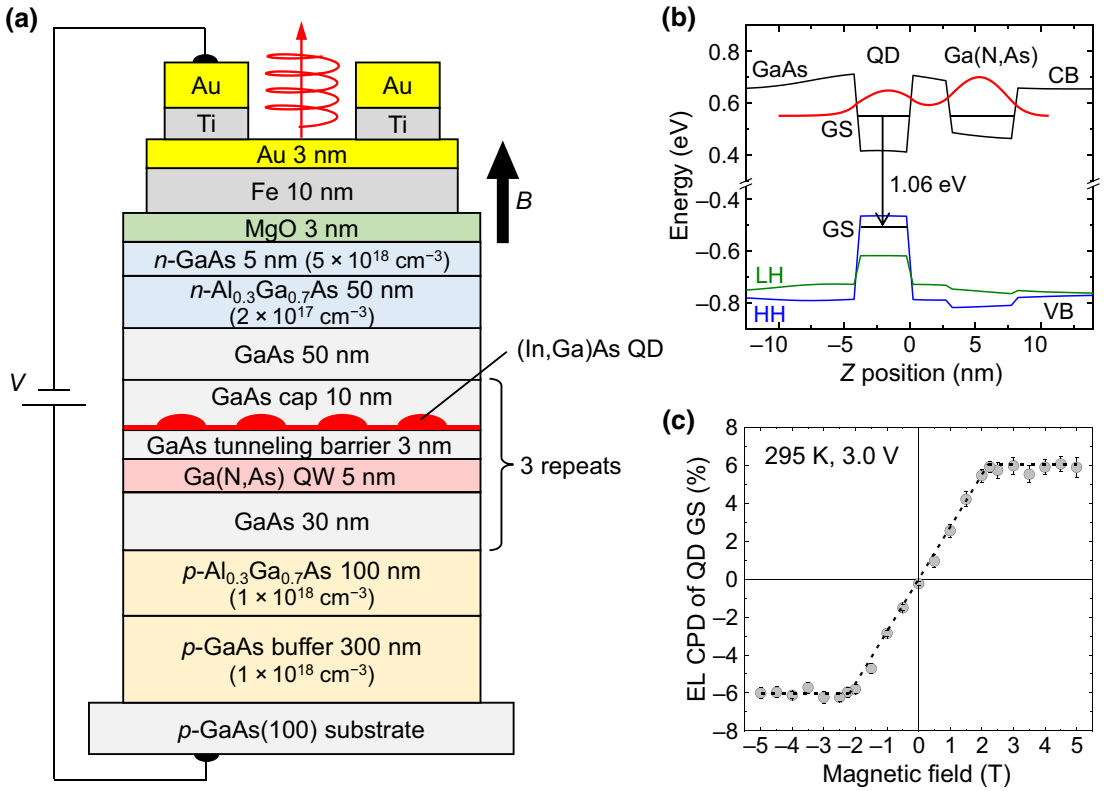

FIG. 1. (a) Schematic of QD spin LED. (b) Three-dimensional calculated band profiles of the tunnel-coupled structure of (In,Ga)As QD and 5-nm-thick Ga(N,As) QW with the coupled electron wave function of the QD GS. (c) Magnetic field dependence of the EL CPD of the QD GS with a bias voltage of 3.0 V at 295 K. Black dashed line indicates the simplified hard-axis magnetization curve of Fe (not experimental data) with a saturation field of 2.2 T [5], which is roughly normalized to the maximum CPD.

Figure 2(a) shows a one-dimensional band structure of the spin LED at different bias voltages calculated using the simulator nextnano [27]. Note that the layer of (In,Ga)As QDs is modeled by a 5-nm-thick (In,Ga)As QW. For semiconductor layers other than the QD layer, the nominal thicknesses, compositions, and doping concentrations are set for the simulation. As reported in a previous study [17], the applied bias drops primarily on the semiconductor layers below 1.5 V and starts to drop on the MgO layer above 1.5 V. However, the applied bias can modify the conduction-band potential of the undoped GaAs barrier, even above 1.5 V. Figures 2(b) and 2(c) show the conduction-band profiles of the undoped GaAs barrier at bias voltages from 2.4 to 3.2 V and the calculated electric field as a function of bias voltage, respectively. Herein, the electric field in GaAs gradually increases with an increase in the bias voltage. When the bias voltage exceeds 2.6 V, the electric field is estimated to be higher than 1 kV/cm. A previous time-resolved PL study revealed that spin polarization in GaAs could be considerably degraded above 1 kV/cm; this is due to DP spin relaxation because of the increase in electron temperature [28]. Therefore, under high-bias conditions, such as 3 V, electron-spin polarization can be greatly reduced during transport in undoped GaAs barriers.

Figures 3(a) and 3(b) show the circularly polarized QD EL spectra and corresponding CPD measured at 2.5 V (40 mA) and 3.0 V (90 mA), respectively, under a magnetic field of 5 T. For comparison, these data measured at 3.0 V (10 mA) for QD spin LED without Ga(N,As) are also shown in Fig. 3(c). Here, the CPD data above 1.17 eV are not shown due to the lack of sufficient EL intensity. Small EL peaks around 1.22 eV are artifacts caused by the liquid-crystal-display backlight. Although Ga(N,As)-derived emission peaks are observed around 1.25 eV for the PL measurements of reference samples with identical QD-Ga(N,As) structures under high excitation power (Fig. S4 within the Supplemental Material [26]), no emission from the Ga(N,As) layer is observed in this EL measurement. This is probably due to the difference in the excited carrier density. Under the EL measurement conditions in this study, conduction-band electrons in Ga(N,As) can be captured in defect states or reinjected into the QDs via wave-function coupling before radiative recombination with holes. For both spin LEDs with and without Ga(N,As), EL peaks appear at approximately 1.06 eV and

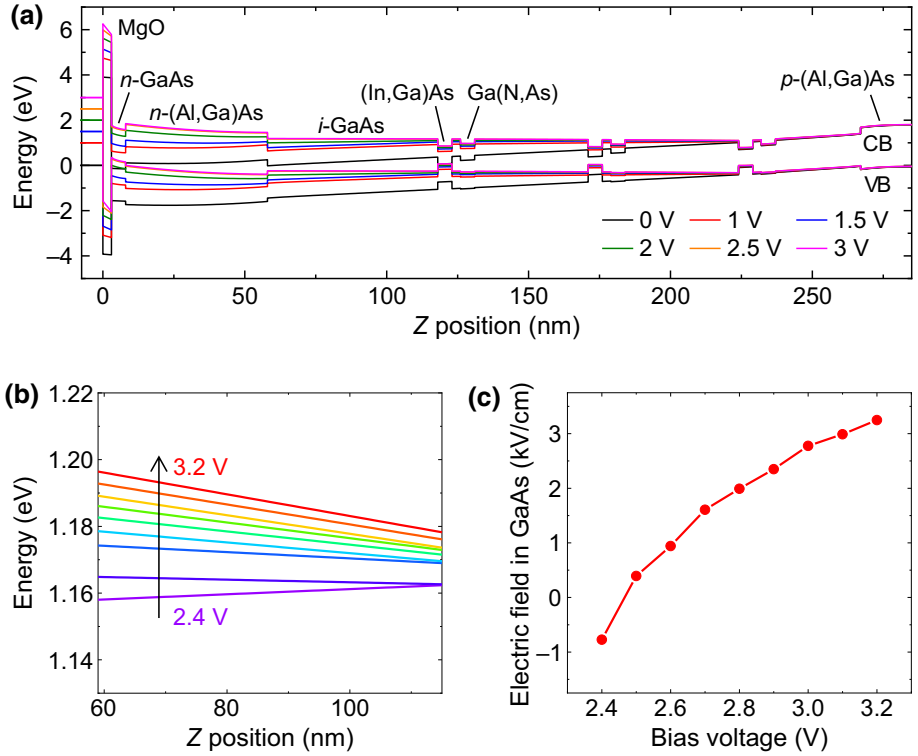

FIG. 2. (a) One-dimensional calculated band structure for spin LED with different bias voltages at 295 K. (b) Conduction-band profiles of undoped GaAs barrier at different bias voltages from 2.4 to 3.2 V for spin LED. (c) Calculated electric field in undoped GaAs barrier as a function of bias voltage.

correspond to light emission from the QD GS, as indicated in Fig. 1(b). We observe no change in the peak energy with bias voltage (Fig. S4 within the Supplemental Material [26]), which indicates that there is no quantum-confined Stark effect [29]. The higher-energy shoulder above 1.10 eV can be attributed to light emission from the QD excited states due to thermal redistribution of carriers [8]. Here, the full width at half maximum of the QD EL band shown in Figs. 3(a) and 3(b) can be estimated as around 80 meV. The broad EL spectra are mainly attributed to the variation in the QD size. The Ga(N,As) QW also has a large energy broadening due to the variation in the nitrogen composition, which is reflected by the broad PL band of the Ga(N,As) QW (Fig. S5 within the Supplemental Material [26]). These facts mean that the density-of-state broadening of electrons in both Ga(N,As) and QDs can result in a wide energy spread for their resonant-energy alignment [25]. Therefore, a large proportion of QDs can have a resonant alignment with the Ga(N,As) spin filter. This is confirmed by almost constant EL CPD with photon energy.

Figure 3(d) shows the integrated QD EL intensity as a function of injection current for the QD spin LED with and without Ga(N,As). For the QD spin LED with Ga(N,As), when the injection current (bias voltage) is increased from 40 mA (2.5 V) to 90 mA (3.0 V), the EL intensity becomes approximately 5 times stronger. In general, for larger injection currents (bias voltages), the transfer time of electrons in semiconductors can be reduced, owing to an increase in the drift speed. This can suppress the possibility of electron trapping by nonradiative defects during transport. Therefore, the large increase in QD EL intensity with injection current stems from the increase in the number of electrons transported to the QDs because of high-speed electron transfer under high electric fields. On the other hand, the operating current for the QD spin LED with Ga(N,As) is much higher than that for the QD spin LED without Ga(N,As). The higher injection current for LED operation (sufficient QD EL emission) is attributed to the tunnel coupling of the QD emitter and Ga(N,As). Electrons injected into the QDs are easily transferred to the Ga(N,As) layer with deep-level defects through wave-function coupling [see Fig. 1(b)], leading to the low electron density of QDs during light emission. This electron transfer from the QD emitter to the Ga(N,As) layer not only significantly reduces the QD EL intensity, but also increases the operating current. The apparent external quantum efficiency (EQE) ratio of QD spin LEDs with Ga(N,As) to that without Ga(N,As) can be estimated as approximately 2%, as deduced from a comparison of the integrated QD EL intensity at 30 mA (Fig. S6 within the Supplemental Material [26]). To improve the EQE, it is effective not only to reduce

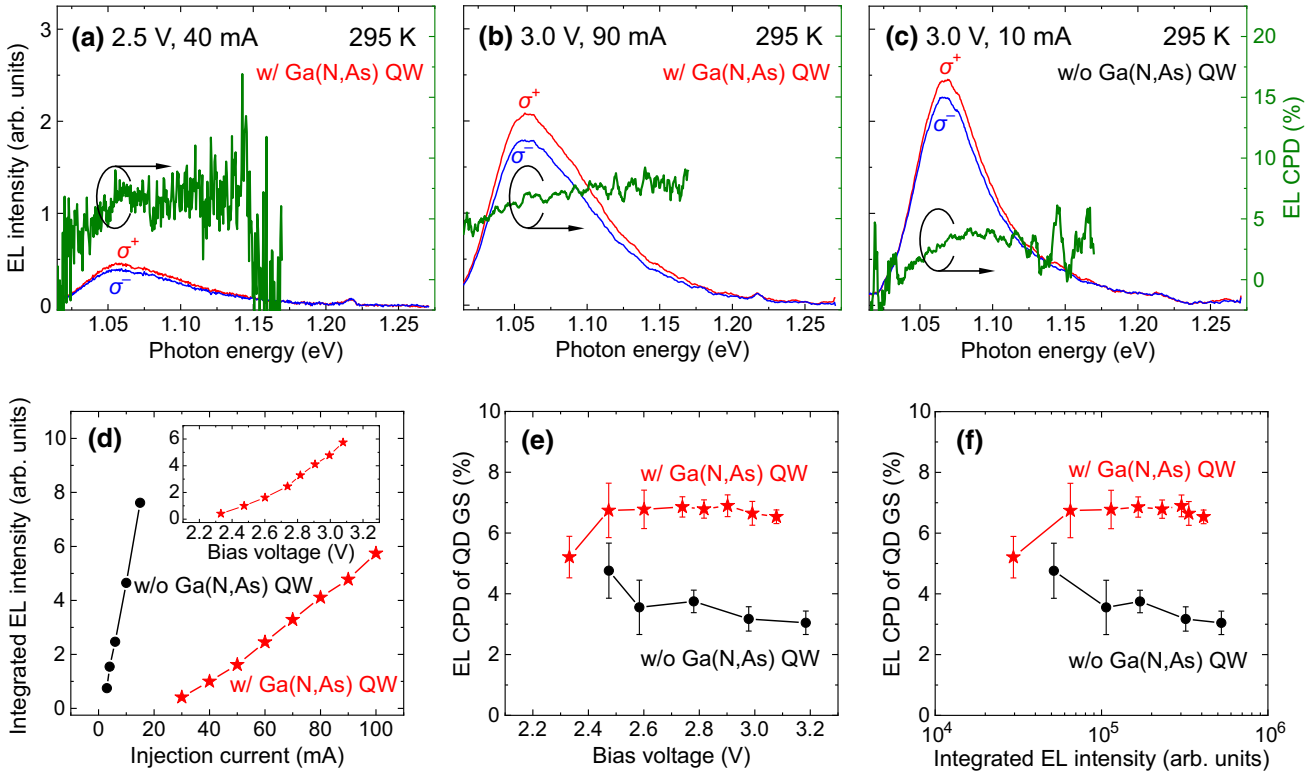

FIG. 3. Circularly polarized QD EL spectra and corresponding CPD measured with (a) 2.5 V (40 mA) and (b) 3.0 V (90 mA) for QD spin LED with Ga(N,As), and (c) 3.0 V (10 mA) for QD spin LED without Ga(N,As) at 295 K under $B = 5$ T. (d) Integrated QD EL intensity as a function of injection current at 295 K under $B = 5$ T for QD spin LED with and without Ga(N,As). Data are normalized to the EL intensity at 40 mA (2.5 V) for QD spin LED with Ga(N,As). Inset shows the integrated QD EL intensity as a function of bias voltage for QD spin LED with Ga(N,As). EL CPD of QD GS as a function of (e) bias voltage and (f) integrated QD EL intensity for QD spin LED with and without Ga(N,As).

the Ga(N,As) QW thickness to increase the internal quantum efficiency, but also to change the tunnel barrier from MgO to GaO_x to increase the electron-injection efficiency [30].

The EL CPD of the QD GS as a function of the bias voltage is shown in Fig. 3(e) for the QD spin LED with and without the Ga(N,As) QW. Here, the QD GS is defined as the energy range of 1.05–1.07 eV. For the conventional QD spin LED without Ga(N,As), the EL CPD decreases from 4.5% at 2.5 V to 3% at 3.0 V. The decrease in the EL CPD with increasing bias voltage can be interpreted based on the acceleration of electric-field-induced DP spin relaxation in undoped GaAs barriers, as discussed in a previous study [17]. In contrast, for the QD spin LED with Ga(N,As), a higher EL CPD of approximately 7% is achieved over a wide bias range from 2.5 to 3.1 V. It should be noted that a high-EL CPD is maintained for a bias of 3 V, at which an electric field higher than 2 kV/cm can be applied to the undoped GaAs layer [see Fig. 2(c)]. This result has significant implications for achieving both strong EL emission and high-EL circular polarization in QD spin LEDs. As shown in Fig. 3(f), the EL CPD for the conventional QD spin LED without Ga(N,As) decreases as the QD EL intensity increases, whereas the EL CPD for the QD spin LED with Ga(N,As) remains high at approximately 7%.

To elucidate the mechanism of the high-EL CPD under high-bias conditions, we perform circularly polarized PL measurements of the QD spin LED with Ga(N,As) under a bias voltage with no magnetic field. Figure 4(a) shows the PL CPD values of the QD GS as a function of bias voltage under the excitation of an undoped GaAs barrier with an excitation power of 6 mW. The EL components are subtracted from measured data to extract the net PL components. The PL CPD of 21% at 2.2 V slightly decreases to 20% at 2.6 V, and then largely decreases to 13% at 3.2 V. The voltage at which the decrease in CPD accelerates agrees well with that of the acceleration of the electric-field-induced DP spin relaxation in undoped GaAs, as deduced from the calculated electric field [see Fig. 2(c)]. Therefore, the larger decrease in PL CPD above 2.6 V originates from the promoted DP spin relaxation in undoped GaAs. These results suggest that electron-spin polarization can be reduced before injection into the QDs under high-bias conditions above 2.6 V.

Figure 4(b) depicts the PL CPD values of the QD GS as a function of excitation power under a high-bias condition

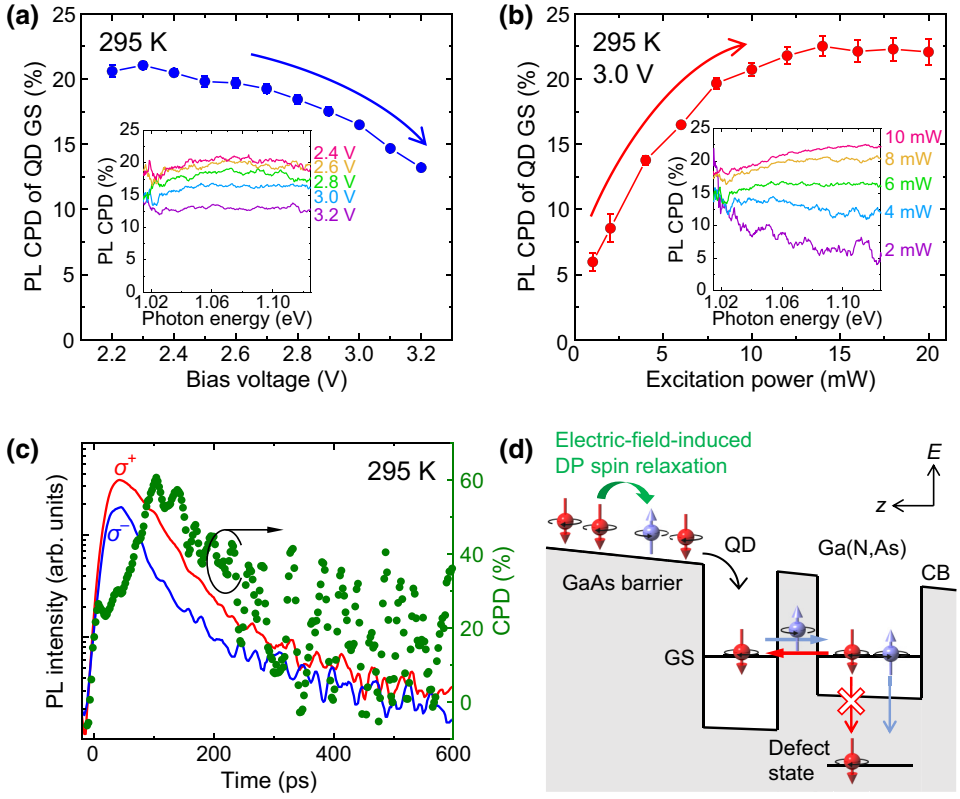

FIG. 4. (a) PL CPD of QD GS at 295 K as a function of bias voltage with an excitation power of 6 mW. Inset shows the PL CPD spectra at different bias voltages with $B = 0$ T under excitation of undoped GaAs barrier. (b) PL CPD of QD GS at 295 K as a function of excitation power at 3.0 V. Inset shows PL CPD spectra at different excitation powers with $B = 0$ T under excitation of undoped GaAs barrier. (c) Circularly polarized PL time profiles and corresponding CPD of QD GS at 295 K for a single layer of (In,Ga)As QDs tunnel coupled with 5-nm-thick Ga(N,As) QW. (d) Simple schematic of the working principle under high-bias conditions for the QD spin LED with Ga(N,As) QW.

of 3.0 V. The PL CPD increases significantly from 6% at 1 mW to a maximum of 23% at 14 mW. For conventional QDs, the PL CPD gradually decreases with increasing excitation power, owing to the state-filling effect in QDs [31–33]. The observed amplification of the electron-spin polarization with excitation power is unique to Ga(N,As) [34]. Here, note that in Fig. 4(a) the increase in only the bias voltage cannot enhance the spin-amplification effect, since the excited electron-spin density is constant in this PL measurement. Figure 4(c) shows the circularly polarized PL time profiles and the corresponding CPD of the QD GS under pulsed σ^+-polarized excitation of GaAs barriers for a single layer of (In,Ga)As QDs tunnel coupled with a 5-nm-thick Ga(N,As) QW grown under identical conditions, without the application of bias voltage. A temporal increase in CPD from the initial value of 25% to a maximum of 60% is observed over the time window from 0 to 100 ps. This CPD amplification is caused by a σ^+ PL decay time that is longer than the σ^- PL decay time. This result indicates efficient removal of minority spins from the QD GS during light emission. Here, the PL rise time can be estimated as approximately 30 ps, which is similar to that of a single-layer sample of (In,Ga)As QDs without Ga(N,As) (Fig. S7 within the Supplemental Material [26]). This result means that the PL rise mainly reflects carrier injection from the GaAs barrier into the QDs. Therefore, the initial CPD of 25% corresponds to the polarization of electron spins directly injected from the GaAs barrier into the QDs. On the other hand, the temporal CPD increase is much slower than the PL rise. The slow CPD amplification should reflect the reinjection of highly polarized electron spins from the Ga(N,As) spin filter to QDs, including a tunneling process. Therefore, we expect that the CPD increase during light emission can be attributed to both efficient removal of minority spins and reinjection of majority spins [25]. The details of a series of processes are discussed below.

Based on the results described above, we discuss the mechanism of high-EL CPD under high-bias conditions. First, highly polarized electron spins are tunnel injected from the Fe electrode into the semiconductor layers. Subsequently, the spin polarization of electrons can be significantly reduced in the undoped GaAs barrier because of the electric-field-induced DP spin relaxation. Next,

electrons with reduced spin polarization are injected into the QDs. However, spin polarization of the QDs can be amplified after injection into the QDs because of the remote spin filtering of QD electrons via an adjacent tunnel-coupled Ga(N,As) QW. As described above, under high-bias conditions (approximately 3.0 V), a number of electron spins are easily transported to the QDs, owing to high-speed electron transfer. In this situation, the injected electron spins are transferred from QDs to Ga(N,As) via strong wave-function coupling [see Fig. 1(b)] and subsequently captured by spin-filtering defects due to thermally accelerated carrier capture [25]. The electron spins transferred to the Ga(N,As) QW are slightly polarized, thus generating spin-polarized defect states. Because such spin-polarized defects capture only conduction-band electrons with the opposite spin direction due to Pauli blocking, the minority spins can be selectively transferred from QDs to Ga(N,As), and the majority spins can be reinjected from Ga(N,As) into QDs, as illustrated in Fig. 4(d). The spin amplification of the Ga(N,As) can be enhanced by increasing the excited electron-spin density, as shown in Fig. 4(b). Based on these results, we can conclude that the injection current (injected electron-spin density) increases as the bias voltage is increased in the EL measurements, which enhances the spin-amplification effect of the Ga(N,As) QW. In contrast, a high-bias voltage can simultaneously promote DP spin relaxation in the undoped GaAs layer, thereby leading to reduced spin polarization of the injected electrons. We anticipate that the trade-off relationship between spin amplification of Ga(N,As) and electric-field-induced DP spin relaxation in the undoped GaAs can result in an almost constant EL CPD of approximately 7% over a wide bias range of 2.5–3.1 V [see Fig. 3(e)].

Finally, we discuss the Ga(N,As) QW position and GaAs tunneling-barrier thickness between the QD and Ga(N,As) QW. Although the Ga(N,As) QW is placed below the QD layer in this study, it is possible to put the Ga(N,As) QW above the QD layer. In that case, the QDs are expected to be tunnel coupled with the Ga(N,As) QW through the GaAs capping barrier. Such a QD-Ga(N,As) coupled structure is undesirable from the point of homogeneous tunnel coupling. In general, since the heights of the embedded QDs vary, the separation distance between the QD and Ga(N,As) QW is different among QDs. This leads to inhomogeneous wave-function coupling between the QD and Ga(N,As) QW. On the other hand, when the Ga(N,As) QW is placed below the QD layer, as in this study, the separation distance is the same for all QDs and the tunnel coupling strength can be varied by changing the GaAs barrier thickness between the QD and Ga(N,As) QW. When the GaAs tunneling-barrier thickness increases, wave-function coupling between the QD and Ga(N,As) QW becomes weaker. In this case, the contribution of the Ga(N,As) spin-filtering layer to spin polarization of the QDs also becomes lower. A previous study found that the optimal value of the GaAs tunneling-barrier thickness for achieving higher spin polarization of QDs was within the range of 3–5 nm [25].

IV. CONCLUSION

The bias dependence of EL circular polarization for a spin LED using a tunnel-coupled structure of (In,Ga)As QDs and Ga(N,As) QW is studied at room temperature. A high-EL circular polarization of approximately 7% is achieved, even under high-bias conditions, despite the high electric field (greater than 2 kV/cm) that this bias induces in the undoped GaAs barriers; in contrast, a lower EL circular polarization of approximately 3% is obtained for the QD spin LED without Ga(N,As). The EL CPD value of approximately 7% corresponds to approximately 18% of the electron-spin polarization of the ferromagnetic Fe electrode. Although the high-bias conditions promote electric-field-induced DP spin relaxation in the undoped GaAs barrier, thereby leading to a decrease in the spin polarization of electrons injected into the QDs, the increase in bias voltage also activates remote spin filtering of QD electrons via an adjacent tunnel-coupled Ga(N,As) QW. Consequently, spin polarization of the QD electrons can be significantly recovered after injection into the QDs. These findings indicate that the active layer, consisting of the QD emissive layer and Ga(N,As) spin filter, is a promising candidate for achieving both strong EL emission and high-EL circular polarization of spin LEDs under high-bias conditions.

ACKNOWLEDGMENTS

This work is financially supported by the Japan Society for the Promotion of Science (JSPS) KAKENHI (Grants No. JP16H06359, No. JP19H05507, No. JP19K15380, No. JP21H01356, and No. JP21KK0068), JST FOREST (Grant No. JPMJFR202E), and Advanced Technology Institute Research Grants 2021. Part of this work is conducted at Hokkaido University, supported by the "Nanotechnology Platform Program" of the Ministry of Education, Culture, Sports, Science and Technology (MEXT), Japan (Grant No. JPMXP09F20HK0010).

[1] B. Jonker, Progress toward electrical injection of spin-polarized electrons into semiconductors, Proc. IEEE **91**, 727 (2003).

[2] F. Meier and B. P. Zakharchenya, *Optical Orientation* (Elsevier, North-Holland, 1984).

[3] R. Fiederling, M. Keim, G. Reuscher, W. Ossau, G. Schmidt, A. Waag, and L. W. Molenkamp, Injection and detection of a spin-polarized current in a light-emitting diode, Nature **402**, 787 (1999).

[4] H. J. Zhu, M. Ramsteiner, H. Kostial, M. Wassermeier, H.-P. Schönherr, and K. H. Ploog, Room-Temperature Spin Injection from Fe into GaAs, Phys. Rev. Lett. **87**, 016601 (2001).

[5] A. T. Hanbicki, B. T. Jonker, G. Itskos, G. Kioseoglou, and A. Petrou, Efficient electrical spin injection from a magnetic metal/tunnel barrier contact into a semiconductor, Appl. Phys. Lett. **80**, 1240 (2002).

[6] V. F. Motsnyi, J. D. Boeck, J. Das, W. V. Roy, G. Borghs, E. Goovaerts, and V. I. Safarov, Electrical spin injection in a ferromagnet/tunnel barrier/semiconductor heterostructure, Appl. Phys. Lett. **81**, 265 (2002).

[7] G. Salis, R. Wang, X. Jiang, R. M. Shelby, S. S. P. Parkin, S. R. Bank, and J. S. Harris, Temperature independence of the spin injection efficiency of a MgO-based tunnel spin injector, Appl. Phys. Lett. **87**, 262503 (2005).

[8] C. H. Li, G. Kioseoglou, O. M. J. van't Erve, M. E. Ware, D. Gammon, R. M. Stroud, B. T. Jonker, R. Mallory, M. Yasar, and A. Petrou, Electrical spin pumping of quantum dots at room temperature, Appl. Phys. Lett. **86**, 132503 (2005).

[9] X. Y. Dong, C. Adelmann, J. Q. Xie, C. J. Palmstrøm, X. Lou, J. Strand, P. A. Crowell, J.-P. Barnes, and A. K. Petford-Long, Spin injection from the Heusler alloy Co_2MnGe into $Al_{0.1}Ga_{0.9}As$/GaAs heterostructures, Appl. Phys. Lett. **86**, 102107 (2005).

[10] X. Jiang, R. Wang, R. M. Shelby, R. M. Macfarlane, S. R. Bank, J. S. Harris, and S. S. P. Parkin, Highly Spin-Polarized Room-Temperature Tunnel Injector for Semiconductor Spintronics Using MgO(100), Phys. Rev. Lett. **94**, 056601 (2005).

[11] L. Lombez, P. Renucci, P. F. Braun, H. Carrère, X. Marie, T. Amand, B. Urbaszek, J. L. Gauffier, P. Gallo, T. Camps, *et al.*, Electrical spin injection into *p*-doped quantum dots through a tunnel barrier, Appl. Phys. Lett. **90**, 081111 (2007).

[12] B. S. Tao, P. Barate, J. Frougier, P. Renucci, B. Xu, A. Djeffal, H. Jaffrès, J.-M. George, X. Marie, S. Petit-Watelot, *et al.*, Electrical spin injection into GaAs based light emitting diodes using perpendicular magnetic tunnel junction-type spin injector, Appl. Phys. Lett. **108**, 152404 (2016).

[13] C. Adelmann, X. Lou, J. Strand, C. J. Palmstrøm, and P. A. Crowell, Spin injection and relaxation in ferromagnet-semiconductor heterostructures, Phys. Rev. B **71**, 121301(R) (2005).

[14] S. H. Liang, *et al.*, Large and robust electrical spin injection into GaAs at zero magnetic field using an ultrathin CoFeB/MgO injector, Phys. Rev. B **90**, 085310 (2014).

[15] A. E. Giba, X. Gao, M. Stoffel, X. Devaux, B. Xu, X. Marie, P. Renucci, H. Jaffrès, J.-M. George, G. Cong, *et al.*, Spin Injection and Relaxation in *p*-Doped (In,Ga)As/GaAs Quantum-Dot Spin Light-Emitting Diodes at Zero Magnetic Field, Phys. Rev. Appl. **14**, 034017 (2020).

[16] A. T. Hanbicki, O. M. J. van't Erve, R. Magno, G. Kioseoglou, C. H. Li, B. T. Jonker, G. Itskos, R. Mallory, M. Yasar, and A. Petrou, Analysis of the transport process providing spin injection through an Fe/AlGaAs Schottky barrier, Appl. Phys. Lett. **82**, 4092 (2003).

[17] K. Etou, S. Hiura, S. Park, K. Sakamoto, J. Takayama, A. Subagyo, K. Sueoka, and A. Murayama, Room-Temperature Spin-Transport Properties in an $In_{0.5}Ga_{0.5}As$ Quantum Dot Spin-Polarized Light-Emitting Diode, Phys. Rev. Appl. **16**, 014034 (2021).

[18] M. Paillard, X. Marie, P. Renucci, T. Amand, A. Jbeli, and J. M. Gérard, Spin Relaxation Quenching in Semiconductor Quantum Dots, Phys. Rev. Lett. **86**, 1634 (2001).

[19] P. Borri, W. Langbein, S. Schneider, U. Woggon, R. Sellin, D. Ouyang, and D. Bimberg, Ultralong Dephasing Time in InGaAs Quantum Dots, Phys. Rev. Lett. **87**, 157401 (2001).

[20] M. Kroutvar, Y. Ducommun, D. Heiss, M. Bichler, D. Schuh, G. Abstreiter, and J. J. Finley, Optically programmable electron spin memory using semiconductor quantum dots, Nature **432**, 81 (2004).

[21] M. Sugawara and M. Usami, Handling the heat, Nat. Photonics **3**, 30 (2009).

[22] Y. Yang, Y. Zheng, W. Cao, A. Titov, J. Hyvonen, J. R. Manders, J. Xue, P. H. Holloway, and L. Qian, High-efficiency light-emitting devices based on quantum dots with tailored nanostructures, Nat. Photonics **9**, 259 (2015).

[23] S. Sato, S. Hiura, J. Takayama, and A. Murayama, Suppression of thermally excited electron-spin relaxation in InGaAs quantum dots using *p*-doped capping layers toward enhanced room-temperature spin polarization, Appl. Phys. Lett. **116**, 182401 (2020).

[24] Y. Puttisong, I. A. Buyanova, and W. M. Chen, Limiting factor of defect-engineered spin-filtering effect at room temperature, Phys. Rev. B **89**, 195412 (2014).

[25] Y. Huang, V. Polojärvi, S. Hiura, P. Höjer, A. Aho, R. Isoaho, T. Hakkarainen, M. Guina, S. Sato, J. Takayama, *et al.*, Room-temperature electron spin polarization exceeding 90% in an opto-spintronic semiconductor nanostructure via remote spin filtering, Nat. Photonics **15**, 475 (2021).

[26] See the Supplemental Material at http://link.aps.org/supplemental/10.1103/PhysRevApplied.19.024055 for secondary-ion mass spectrometry from three layers of 20-nm-thick Ga(N,As), atomic force microscopy and transmission electron microscopy analysis of reference QDs, EL spectra under various bias voltages, PL spectra of QD samples with Ga(N,As) QWs, comparison of QD EL intensity between QD spin LEDs with and without Ga(N,As), and a comparison of PL rise time for (In,Ga)As QD samples with and without Ga(N,As).

[27] S. Birner, T. Zibold, T. Andlauer, T. Kubis, M. Sabathil, A. Trellakis, and P. Vogl, Nextnano: General purpose 3-D simulations, IEEE Trans. Electron Devices **54**, 2137 (2007).

[28] H. Sanada, I. Arata, Y. Ohno, Z. Chen, K. Kayanuma, Y. Oka, F. Matsukura, and H. Ohno, Relaxation of photoinjected spins during drift transport in GaAs, Appl. Phys. Lett. **81**, 2788 (2002).

[29] D. A. B. Miller, D. S. Chemla, T. C. Damen, A. C. Gossard, W. Wiegmann, T. H. Wood, and C. A. Burrus, Band-Edge Electroabsorption in Quantum Well Structures: The Quantum-Confined Stark Effect, Phys. Rev. Lett. **53**, 2173 (1984).

[30] H. Saito, J. C. Le Breton, V. Zayets, S. Yuasa, and K. Ando, Highly enhanced electron-injection efficiency in GaAs-based light-emitting diodes using a Fe/GaO_x tunnel injector, Appl. Phys. Express **2**, 083003 (2009).

[31] S. Hiura, K. Takeishi, M. Urabe, K. Itabashi, J. Takayama, T. Kiba, K. Sueoka, and A. Murayama, Interdot spin transfer dynamics in laterally coupled excited spin ensemble of high-density InGaAs quantum dots, Appl. Phys. Lett. **113**, 023104 (2018).

[32] S. Hiura, S. Saito, J. Takayama, T. Kiba, and A. Murayama, Layer-selective spin amplification in size-modulated quantum nanocolumn, Appl. Phys. Lett. **115**, 013102 (2019).

[33] S. Hiura, S. Hatakeyama, J. Takayama, and A. Murayama, Asymmetric spin relaxation induced by residual electron spin in semiconductor quantum-dot-superlattice hybrid nanosystem, Appl. Phys. Lett. **116**, 262407 (2020).

[34] X. J. Wang, I. A. Buyanova, F. Zhao, D. Lagarde, A. Balocchi, X. Marie, C. W. Tu, J. C. Harmand, and W. M. Chen, Room-temperature defect-engineered spin filter based on a non-magnetic semiconductor, Nat. Mater. **8**, 198 (2009).